The rate of DNA evolution: Effects of body size and temperature on the molecular clock

James F. Gillooly*†, Andrew P. Allen*, Geoffrey B. West‡§, and James H. Brown*‡

*Department of Biology, University of New Mexico, Albuquerque, NM 87131; ‡Santa Fe Institute, 1399 Hyde Park Road, Santa Fe, NM 87501; and §Theoretical Physics Division, Los Alamos National Laboratory, MS B285, Los Alamos, NM 87545

Communicated by Murray Gell-Mann, Santa Fe Institute, Santa Fe, NM, November 9, 2004 (received for review March 26, 2004)

Observations that rates of molecular evolution vary widely within and among lineages have cast doubts on the existence of a single ''molecular clock.'' Differences in the timing of evolutionary events estimated from genetic and fossil evidence have raised further questions about the accuracy of molecular clocks. Here, we present a model of nucleotide substitution that combines theory on metabolic rate with the now-classic neutral theory of molecular evolution. The model quantitatively predicts rate heterogeneity and may reconcile differences in molecular- and fossil-estimated dates of evolutionary events. Model predictions are supported by extensive data from mitochondrial and nuclear genomes. By accounting for the effects of body size and temperature on metabolic rate, this model explains heterogeneity in rates of nucleotide substitution in different genes, taxa, and thermal environments. This model also suggests that there is indeed a single molecular clock, as originally proposed by Zuckerkandl and Pauling [Zuckerkandl, E. & Pauling, L. (1965) in *Evolving Genes and Proteins*, eds. Bryson, V. & Vogel, H. J. (Academic, New York), pp. 97–166], but that it ''ticks'' at a constant substitution rate per unit of mass-specific metabolic energy rather than per unit of time. This model therefore links energy flux and genetic change. More generally, the model suggests that body size and temperature combine to control the overall rate of evolution through their effects on metabolism.

mutation | metabolic theory | allometry | substitution

Completion of the modern evolutionary synthesis will require better understanding of the molecular processes of evolutionary change. The speed of molecular evolution can be measured as the rate of genetic divergence of descendants from a common ancestor, so the rate of molecular evolution can be quantified in terms of the changes in the nucleotide sequences that comprise the genome. Observations that rates of molecular evolution vary widely within and among lineages have raised doubts about the existence of a single ''molecular clock,'' as originally proposed by Zuckerkandl and Pauling (1). The accuracy of molecular clocks is further called into question because molecular estimates of divergence time often disagree with the fossil record (2, 3). Understanding the factors responsible for rate heterogeneity is key to resolving differences between molecular and fossil-based estimates of important evolutionary events [e.g., Cambrian explosion (4, 5) and proliferation of modern mammalian orders (2)]. More generally, understanding rate heterogeneity may yield insight into the factors affecting overall rates of evolution.

Variations in rates of nucleotide substitution have been correlated with body size, metabolic rate (6), generation time (7), and environmental temperature (8, 9). Differences also have been observed between endotherms and ectotherms (6, 10). This rate heterogeneity most often is attributed to one of two causes, metabolic rate or generation time. According to the metabolic rate hypothesis, most mutations are caused by genetic damage from free radicals produced as byproducts of metabolism, so mutation rates should be related to cellular or mass-specific metabolic rates (6). According to the generation time hypothesis, most mutations are caused by errors in DNA replication during cell division, so mutation rates should be related to the number of divisions in germ cell lines and hence to generation times (7). Distinguishing between these hypotheses has been difficult because free radical production and generation time both vary with metabolic rate (6, 11), which in turn varies with body size and temperature (12).

Here, we propose a model that predicts heterogeneity in rates of molecular evolution by combining principles of allometry and biochemical kinetics with Kimura's neutral theory of evolution. The model quantifies the relationship between rates of energy flux and genetic change based explicitly on the effects of body size and temperature on metabolic rate. Although the model does not distinguish between the metabolic rate and generation time hypotheses, it accounts for much of the observed rate heterogeneity across a wide range of taxa in diverse environments. Recalibrating the molecular clocks by using metabolic rate reconciles some fossil- and molecular-based estimates of divergence.

The Model

Metabolic rate is the rate at which energy and materials are taken up from the environment and used for maintenance, growth, and reproduction. It ultimately governs most biological rate processes, including the two generally thought to control mutation rate: free radical production rate and generation time (6, 7, 12, 13). Metabolic rate likely affects other processes, such as DNA repair and environmentally induced mutagenesis, that influence rates of nucleotide substitution (6). Mass-specific metabolic rate (B) varies with body size, M, and temperature, T, as

$$B = b_o M^{-1/4} e^{-E/kT}, \quad [1]$$

where b_o is a coefficient independent of body size and temperature (12). The body size term, $M^{-1/4}$, has its origins in the fractal-like geometry of biological exchange surfaces and distribution networks (14). The Boltzmann or Arrhenius factor, $e^{-E/kT}$, underlies the temperature dependence of metabolic rate, where E is an average activation energy for the biochemical reactions of metabolism ($\approx$0.65 eV) (12), k is Boltzmann's constant (8.62×10^{-5} eV·K^{-1}), and T is absolute temperature in degrees Kelvin. Eq. **1** explains most of the variation in the metabolic rates of plants, animals, and microbes (12).

When combined with assumptions of the neutral theory (15), Eq. **1** also can be used to characterize rates of molecular evolution. The first assumption is that molecular evolution is caused primarily by neutral mutations that randomly drift to fixation in a population, resulting in nucleotide substitutions (15). This assumption is consistent with theory and data demonstrating that deleterious mutations have only a negligible chance of becoming fixed in a population because of purifying selection (16), and that favorable mutations occur very rarely

Abbreviation: My, millions of years.

†To whom correspondence should be addressed. E-mail: gillooly@unm.edu.

www.pnas.org/cgi/doi/10.1073/pnas.0407735101

(17). Under this assumption, the rate of nucleotide substitution per generation is equal to the neutral mutation rate per generation and is independent of population size (15). The second assumption is that point mutations, and therefore substitutions, occur at a rate proportional to B. This idea assumes that most mutations are caused by some combination of free radical damage, replication errors, and other processes that ultimately are consequences of metabolism. Together, these two assumptions imply that the nucleotide substitution rate, α, defined as the number of substitutions per site per unit time, varies with body size and temperature as

$$\alpha = f\nu B = f\nu b_o M^{-1/4} e^{-E/kT}, \quad [2]$$

where f is the proportion of point mutations that are selectively neutral, and ν is the number of point mutations per site per unit of metabolic energy expended by a unit mass of tissue (g mutations site^{-1}·J^{-1}). Thus, the product $f\nu$ is the neutral mutation rate per unit of mass-specific metabolic energy and, following Kimura's neutral theory, the substitution rate (see *Appendix 1*, which is published as supporting information on the PNAS web site). If the body size and temperature dependence of substitution rate is controlled by B, then $f\nu$ is predicted to be a constant independent of M and T. Consequently, Eq. **2** predicts the existence of a molecular clock that "ticks" at a constant rate per unit of mass-specific metabolic energy flux rather than per unit of time. On average, a certain quantity of metabolic energy transformation within a given mass of tissue causes a substitution in a given gene regardless of body size, temperature, or taxon. Eq. **2** therefore predicts a 100,000-fold increase in substitution rates across the biological size range ($\approx 10^8$ g of whales to $\approx 10^{-12}$ g of microbes) and a 34-fold increase in substitution rates across the biological temperature range (≈0–40°C).

Rearranging terms in Eq. **2** and taking logarithms yields:

$$\ln(\alpha M^{1/4}) = -E\left(\frac{1}{kT}\right) + C \quad [3]$$

or

$$\ln(\alpha e^{E/kT}) = -1/4 \ln M + C, \quad [4]$$

where $C = \ln(f\nu b_o)$.

Model Predictions

Eqs. **3** and **4** correct for mass and temperature, respectively, and lead to three explicit predictions. The first prediction is that the logarithms of mass-corrected substitution rates should be linear functions of $1/kT$ with slopes of $-E \approx -0.65$ eV (Eq. **3**), reflecting the kinetics of aerobic metabolism. The second prediction is that the logarithms of temperature-corrected substitution rates should be linear functions of $\ln M$ with slopes of approximately $-1/4$ (Eq. **4**), reflecting the allometric scaling of mass-specific metabolic rate (14). Finally, if these first two predictions hold, then the third prediction is that, for a given gene, the number of substitutions per site per unit mass-specific metabolic energy, $f\nu$, should be approximately invariant across taxa.

Methods

Calculation of Substitution Rates. Estimated rates of substitution, α, were compiled from multiple published sources for mitochondrial and nuclear genomes (respectively, *Appendixes 2* and *3*, which are published as supporting information on the PNAS web site). Together, these data represent several major taxonomic groups (e.g., invertebrates, fish, amphibians, reptiles, birds, and mammals), which span 10 orders of magnitude in body size and the biological temperature range 0°C to 40°C. Sequence divergence, D, was estimated by using direct sequencing methods for all sequences considered here except for the entire mitochondrial genome, where the restriction fragment length polymorphism technique was used. For the mitochondrial genome, estimates of sequence divergence were from four different coding regions (12s rRNA, 16s RNA, cytochrome *b*, and whole genome). For the nuclear genome, estimates of sequence divergence were from two published sources based on rates of silent substitution in coding regions. In the first source, divergence estimates were calculated for 11 pairs of primates based on globin gene data (6). In the second source, estimates were obtained for 23 pairs of mammalian taxa that encompass 17,208 protein-coding DNA sequences from 5,669 nuclear genes and 326 species (18) (*Appendix 3*).

Times of divergence, τ in millions of years (My), were independently estimated by using paleontological data (e.g., fossil records and geological events), and varied by ≈2 orders of magnitude for the mitochondrial data (0.43–38 My) and 1 order of magnitude for the nuclear data (5.5–56.5 My) (*Appendixes 2* and *3*). Substitution rates were then calculated as $\alpha = D/2\tau$, which are the average for the two lineages over time τ (*Appendix 4*, which is published as supporting information on the PNAS web site). Although not all sources used the same mathematical model to estimate D in mitochondrial genomes, variation caused by differences in methodology is small (19) compared with the predicted effects of body size and temperature.

Body Size and Temperature Estimates. The formula for estimating substitution rate ($\alpha = D/2\tau$) is an average for two descendent lineages that may differ in body mass. To account for differences in substitution rates caused by differences in body mass between the two lineages, we take the "quarter-power average," which controls for the greater influence of the smaller, more rapidly evolving lineage on the calculated substitution rate (*Appendix 4*). Body temperatures of endothermic birds and mammals were estimated from the literature and varied between ≈35°C and 40°C. Body temperatures of ectotherms were estimated as the mean annual ambient temperature where the organisms presently occur, or in the case of some fishes, the temperature of the preferred habitat. This estimation assumes that extant ectotherms are approximately in thermal equilibrium with their environment, and that they occur in a similar thermal environment as their ancestors.

Assessing Effects of Body Mass and Temperature. Our methods for estimating body size and temperature likely introduce substantial error into these predictor variables. This violates the assumptions of type I regression (20). We therefore used type II regression to assess the quantitative effects of body size and temperature on substitution rates. However, before fitting type II regression models, we first determined whether body size and temperature had significant independent effects on substitution rates. This process was necessary because, for the data considered here, the largest animals all are endotherms, resulting in a positive correlation between body size and temperature. We therefore fitted type I multiple regression models for all of the data shown below. For the mitochondrial data that includes both ectotherms and endotherms, we fitted a model of the form $\ln(\alpha) = \beta \ln(M) - E(1/kT) + C$, and for the mammalian nuclear data, we fitted a model of the form $\ln(\alpha) = \beta \ln(M) + C$. This procedure simultaneously estimates the allometric scaling exponent, β, and activation energy, E, of substitution rates. Multiple regression analyses indicated significant independent effects for body size and temperature ($P < 0.05$) for all data except those for cytochrome *b* data shown in Figs. 1*C* and 2*C*. We note, however, that, on average, the type I regression coefficients were lower than the predicted values of -0.25 for β ($\bar{\beta} = -0.16$, $n = 6$) and 0.65 eV for E ($\bar{E} = 0.40$ eV, $n = 4$) (see *Appendix 4*).

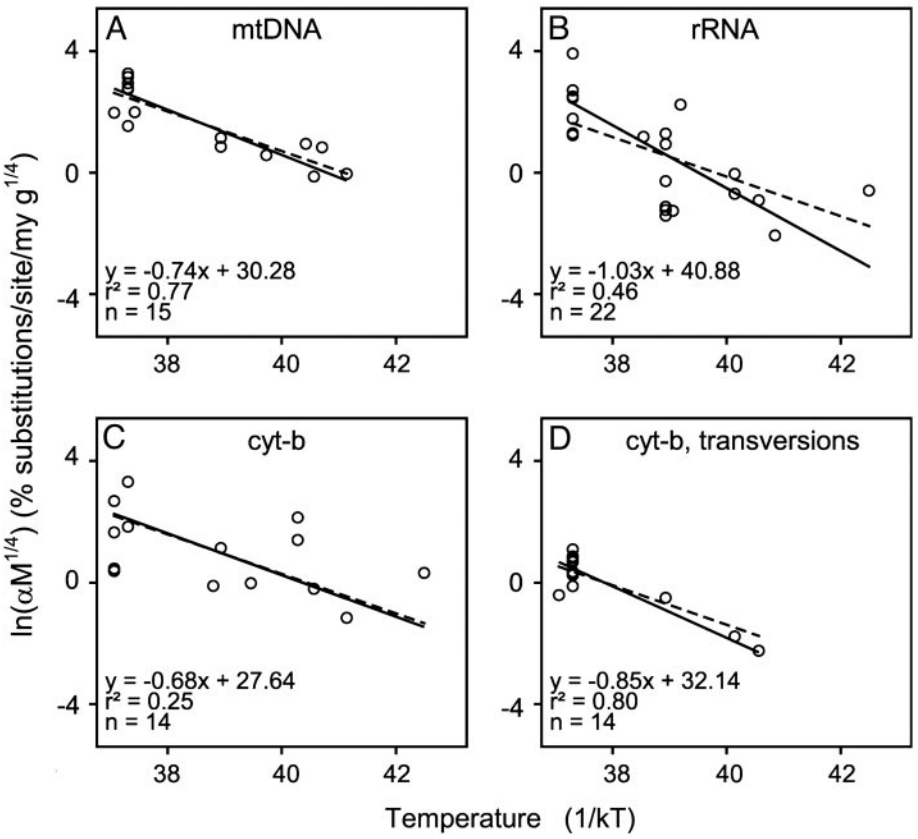

Fig. 1. Effect of temperature on nucleotide substitution rates after correcting for body mass by using Eq. **3**. Plots show four commonly used molecular clocks: the mitochondrial genome (mtDNA) (*A*), rRNA (12s and 16s combined) (*B*), all substitutions in the cytochrome *b* gene (*C*), and transversions in the cytochrome *b* gene (*D*). The solid lines were fitted by using type II linear regression; the dashed lines show the predicted slope of −0.65 eV. Data and sources are listed in *Appendix 2*.

Results and Discussion

Data support each of the model's three predictions. First, the logarithm of mass-corrected substitution rate is a linear function of inverse absolute temperature for the four molecular clocks from the mitochondrial genome (Fig. 1). Temperature accounts for 25–80% of the variation in mass-corrected substitution rates among diverse organisms, including endotherms (body temperatures of ≈35–40°C) and ectotherms from a broad range of thermal environments (≈0–30°C). The type II regression slopes of these lines all are close to the predicted value of −0.65 eV based on the kinetics of metabolism (Table 1). Thus, contrary to some recent reports (21), our results, which incorporated a wide range of body temperatures, indicate that nucleotide substitution rates are strongly temperature-dependent. Second, log-log plots of temperature-corrected substitution rates versus body mass all are well fitted by straight lines (r^2 = 0.23–0.74) for these four clocks, and the slopes all are close to the predicted value of −1/4 (Fig. 2 and Table 1). Substitution rates therefore show the same $M^{-1/4}$ allometric scaling as mass-specific metabolic rate B. Third, both endotherms and ectotherms (vertebrates and invertebrates) fall on the same lines in these relationships, supporting the prediction that $f\nu$ is approximately invariant across taxa for a given gene. Building on previous work showing correlations of substitution rate to body size (6), these results show that all animals cluster around a single line that is predicted by our model. Note that the model quantifies the combined effects of body size and temperature. Analyses that consider these variables separately, like much of the previous literature, explain much less of the observed variation in substitution rates (Table 2).

Still further support for the predicted mass dependence of molecular evolution (prediction 2) comes from analysis of two data sets on rates of silent substitutions in coding sequences of mammalian nuclear genomes. For globin data in primates, a log-log plot of substitution rate versus body mass gives a straight line with a slope close to the predicted value of −1/4 (−0.27, 95% confidence interval: −0.20 to −0.34; r^2 = 0.85, Fig. 3*A*). For a broader assortment of mammals and sequences (*Appendix 3*), a log-log plot also gives a straight line with a slope close to the predicted value of −1/4 (−0.21, 95% confidence interval: −0.18 to −0.23; r^2 = 0.77, Fig. 3*B*). And as predicted, both lines show very similar intercepts (24.79 and 24.81). Thus, it appears that mammalian nuclear genomes have slopes for the mass dependence of substitution rates that are similar to those observed in mitochondrial genomes for a broader range of taxa (Fig. 2), but intercepts which are slightly lower. We note, however, that in Figs. 1–3, observed values deviated by as much as 2.7-fold from the predicted values (Table 1). This residual variation likely indicates the importance of factors other than body size and temperature that affect measured substitution rates. Yet, these deviations of up to 2.7-fold are small compared with the ≈100-fold variation explained by our model.

The fact that the model predicts empirically observed substitution rates supports the hypothesis that there is a direct relationship between the rate of energy transformation in metabolism and the rate of nucleotide substitution. The number of substitutions per site per unit of mass-specific metabolic energy, $f\nu$, can be calculated from the y-intercepts (C) in Figs. 1–3: $f\nu = e^C/b_o$ (Eqs. **3** and **4**). Taking the fitted intercept of $C \approx 26$ for mtDNA (Table 1), and $b_o = 1.5 \times 10^8$ W·g$^{-3/4}$ (12), we obtain

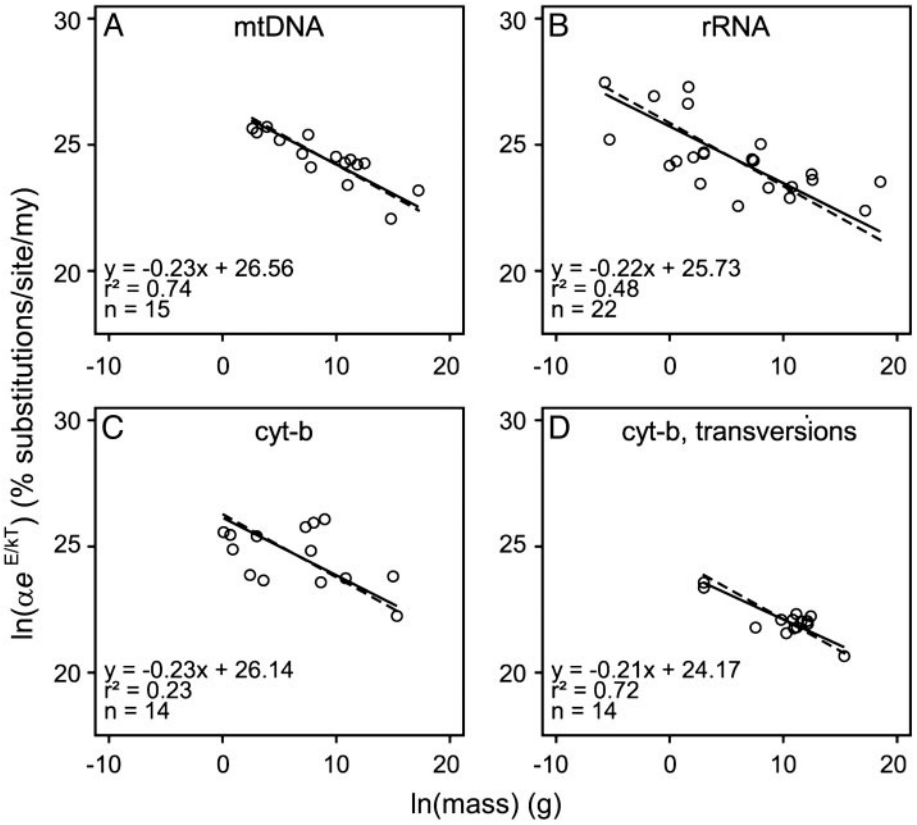

Fig. 2. Effect of body mass on nucleotide substitution rates after correcting for temperature by using Eq. **4**. Plots show the same data from the same four molecular clocks as in Fig. 1. The solid lines were fitted by using type II linear regression; the dashed lines show the predicted slope of $-1/4$. Data and sources are listed in *Appendix 2*.

$f\nu \approx 4 \times 10^{-13}$ g·substitutions·site^{-1}·J^{-1}. Thus, $\approx 2.4 \times 10^{12}$ J of energy must be fluxed per g of tissue to induce one substitution per site in the mitochondrial genome.

Differences in the fitted intercepts, and therefore $f\nu$, among genes, genomes, and types of substitutions may reflect the influence of other factors in addition to body size and temperature. For example, f is known to vary from near 1 for synonymous codon sites and noncoding regions to near 0 for nonsynonymous sites, and ν differs between mitochondrial and nuclear genomes (19). The model could be fine-tuned to incorporate these and other possible sources of variation. In Table 1, the calculated intercepts for overall rates of substitution for mtDNA, rRNA, and cytochrome *b* are all ≈26. The intercept for cytochrome *b* transversions is lower (24.61), as are those for silent nuclear substitutions (24.79 and 24.81). These differences are consistent with current theory and data finding lower rates of transversions than transitions and lower overall rates of substitution in nuclear than in mitochondrial genomes (19).

We illustrate some of the evolutionary implications of this model with three examples. First, Fig. 4 shows estimates of a proposed molecular clock for mammalian divergence times (18), some of which differ substantially from fossil-based estimates. Molecular and fossil-based estimates are in close agreement for humans and chimpanzees (*Homo* and *Pan*, 5.5 My) because the clock calibrated in ref. 18 was disproportionately influenced by

Table 1. Parameter estimates and 95% confidence intervals (95% CI) for type II regression models depicted as solid lines in Figs. 1–3

	$\ln(\alpha M^{1/4})$ vs. $1/kT$		$\ln(\alpha e^{E/kT})$ vs. $\ln(M)$			
Gene/genome	Fitted slope (95% CI)	Predicted slope	Fitted slope (95% CI)	Predicted slope	Calculated intercept	Average residuals
mtDNA	−0.74 (−0.58, −0.90)	−0.65	−0.23 (−0.16, −0.31)	−0.25	26.71	1.6
rRNA	−1.03 (−0.66, −1.41)	−0.65	−0.22 (−0.15, −0.30)	−0.25	25.87	2.7
Cytochrome *b*	−0.68 (−0.42, −0.95)	−0.65	−0.23 (−0.16, −0.30)	−0.25	26.28	2.7
Cytochrome *b* transversions	−0.85 (−0.74, −0.95)	−0.65	−0.21 (−0.17, −0.24)	−0.25	24.61	1.4
Globin, primates			−0.27 (−0.20, −0.34)	−0.25	24.62	1.2
silent nuclear, various mammals			−0.21 (−0.18, −0.23)	−0.25	25.22	1.3
Average	−0.83	−0.65	−0.23	−0.25		1.8

The first four molecular clocks listed are from the mitochondrial genome, the last two are from the nuclear genome. Slopes and intercepts are calculated based on the predicted size and temperature dependence in Eq. **2** and are depicted as dashed lines in the figures. The average residual deviation for each gene or genome shown in Figs. 1–3 is listed in the final column. Average residuals were calculated by averaging the absolute deviations from the dashed lines in Figs. 1–3, and then converting these logarithmic averages to arithmetic values.

Table 2. A comparison of the correlations (r^2 values) of mitochondrial nucleotide substitution rates (α, % substitutions per site per My) versus temperature ($1/kT$) and the natural logarithm of body mass (g) without correction for body mass and temperature, and after correction by using Eqs. 3 and 4

	$\ln(\alpha)$ vs. $1/kT$		$\ln(\alpha)$ vs. $\ln(M)$	
Gene/genome	Uncorrected	Mass corrected	Uncorrected	Temperature corrected
mtDNA	0.23	0.77	0.14	0.74
rRNA	0.03	0.46	0.13	0.48
Cytochrome *b*	0.13	0.25	0.09	0.23
Cytochrome *b* transversions	0.16	0.80	0.00	0.72

the preponderance of data for these and other similarly large mammals. However, their clock-estimated divergence date for Hystricognath rodents predates the fossil estimate by >2-fold (115 My vs. 56.5 My), and for the much smaller rodent genera *Mus* and *Rattus* by >3-fold (41 My vs. 12.5 My). Our model largely reconciles these discrepancies by incorporating the effects of body size and obtaining a date close to the fossil estimate (Fig. 4; we corrected only for mass, because these mammals have similar body temperatures). The procedure of taking the quarter-power average corrects for the greater influence of smaller taxa on rates of divergence because of their higher mass-specific metabolic rates (see *Appendix 4*).

Second, our model suggests how differences in body size might explain the "hominoid slowdown hypothesis," which proposed that rates of molecular evolution have slowed in hominoids since their split from Old World monkeys (22). Based on differences in average body mass between extant hominoids (50 kg) and Old World monkeys (7 kg), our model predicts a ≈0.6-fold slowdown [$=(7\text{ kg}/50\text{ kg})^{1/4}$], close to the estimated 0.7 (22).

Third, our model suggests that differences in temperature may account for the nearly 4-fold discrepancy between a molecular and a geological estimate of the age of notothenioid antarctic fishes (11 My vs. 38 My) (23). Assuming that the temperate-zone ectotherms used to calibrate the clock occurred at ≈15°C, whereas the notothenioid fishes occurred at ≈0°C, our model appears to reconcile this discrepancy ($e^{-E/k(273+15)}/e^{-E/k(273+0)} \approx 4$). These three examples illustrate how calibrating molecular clocks for body size and temperature may provide insights into evolutionary history. Metabolic rates of plants and microbes show similar body size and temperature dependence as animals (12). We expect that the theory developed here should be applicable to these organisms. This expectation is supported by a recent study showing the temperature dependence of mutation rates in plants (9).

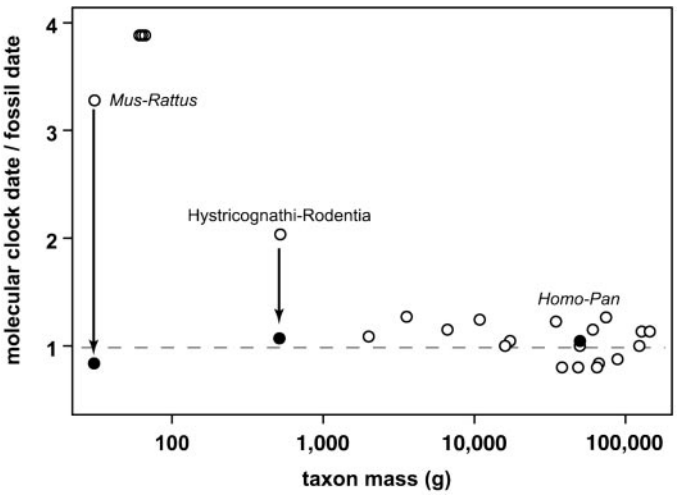

Fig. 4. Correcting for body size gives estimates of divergence dates that agree more closely with the fossil record (see *Appendix 3*). Open circles represent molecular clock estimates of divergence before accounting for effects of body size (18), and closed circles represent molecular clock estimates of divergence after accounting for effects of body size. Mass-corrected divergence dates were estimated by using the regression model in Fig. 3*B*. Arrows connect pairs of mass-corrected and uncorrected estimates, except for *Homo-Pan*, where these estimates are effectively indistinguishable. Correcting for mass has a much greater effect on clock-estimated divergences of small mammals, such as the rodent pair *Mus-Rattus*, because the uncorrected molecular clock in ref. 18 was calibrated mostly with large mammals. The horizontal, dashed line represents equality between molecular and fossil estimates.

These results also may have broader implications for understanding the factors controlling the overall rate of evolution. The central role of metabolic rate in controlling biological rate processes implies that metabolic processes also govern evolutionary rates at higher levels of biological organization where the neutral molecular theory does not apply. So, for example, the rate and direction of phenotypic evolution ultimately depends on the somewhat unpredictable action of natural selection. However, the overall rate of evolution ultimately is constrained by the turnover rate of individuals in

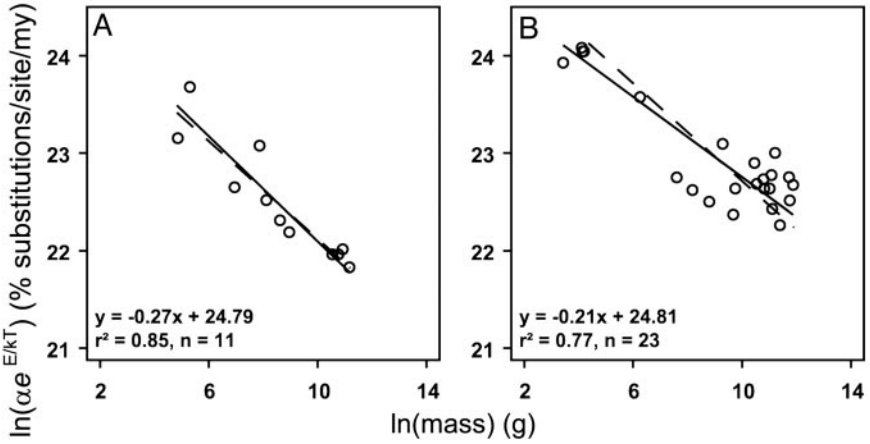

Fig. 3. Effect of body mass on silent rates of nucleotide substitution (% substitutions per site per My) in coding regions of the globin gene in primates (*A*) (6) and multiple coding regions of the nuclear genome for 23 pairs of mammalian lineages (*B*) (ref. 18 and *Appendix 3*).

populations, as reflected in generation time, and the genomic variation among individuals, as reflected in mutation rate (16, 24). Both of these rates are proportional to metabolic rate, so Eq. **1** also may predict the effects of body size and temperature on overall rates of genotypic and phenotypic change. Such predictions would be consistent with general macroevolutionary patterns showing that most higher taxonomic groups originate in the tropics where temperatures are high (25), speciation rates decrease with decreasing temperature from the equator to the poles (26, 27), biodiversity is highest in the tropics (28), and smaller organisms evolve faster and are more diverse than larger organisms (29).

We thank F. Allendorf, E. Charnov, H. Olff, V. Savage, T. Turner, and W. Woodruff for comments or discussions that improved this manuscript and S. Kumar for providing us with his data. J.F.G., G.B.W., and J.H.B. acknowledge support of the Thaw Charitable Trust and a Packard Interdisciplinary Science Grant. G.B.W., A.P.A., and J.H.B. were supported by the National Science Foundation. G.B.W. acknowledges the hospitality of the Mathematics Department at Imperial College, London, and the support of the Engineering and Physical Sciences Research Council.

1. Zuckerkandl, E. & Pauling, L. (1965) in *Evolving Genes and Proteins*, eds. Bryson, V. & Vogel, H. J. (Academic, New York), pp. 97–166.
2. Alroy, J. (1999) *Syst. Biol.* **48,** 107–118.
3. Smith, A. B. & Peterson, K. J. (2002) *Annu. Rev. Earth Planetary Sci.* **30,** 65–88.
4. Wray, G. A., Levinton, J. S. & Shapiro, L. H. (1996) *Science* **274,** 568–573.
5. Ayala, F. J., Rzhetsky, A. & Ayala, F. J. (1998) *Proc. Natl. Acad. Sci. USA* **95,** 606–611.
6. Martin, A. P. & Palumbi, S. R. (1993) *Proc. Natl. Acad. Sci. USA* **90,** 4087–4091.
7. Laird, C. D., McConaughty, B. L. & McCarthy, B. J. (1969) *Nature* **224,** 149–154.
8. Bleiweiss, R. (1998) *Proc. Natl. Acad. Sci. USA* **95,** 612–616.
9. Wright, S. D., Gray, R. D. & Gardner, R. C. (2003) *Evolution* **57,** 2893–2898.
10. Rand, D. M. (1994) *Trends Ecol. Evol.* **9,** 125–131.
11. Savage, V. M., Gillooly, J. F., Brown, J. H., West, G. B. & Charnov, E. L. (2004) *Am. Nat.* **163,** E429–E441.
12. Gillooly, J. F., Brown, J. H., West, G. B., Savage, V. M. & Charnov, E. L. (2001) *Science* **293,** 2248–2251.
13. Gillooly, J. F., Charnov, E. L., West, G. B., Savage, V. M. & Brown, J. H. (2002) *Nature* **417,** 70–73.
14. West, G. B., Brown, J. H. & Enquist, B. J. (1997) *Science* **276,** 122–126.
15. Kimura, M. (1968) *Nature* **217,** 624–626.
16. Fisher, R. A. (1930) *The Genetical Theory of Natural Selection* (Clarendon, Oxford).
17. Dobzhansky, T. (1951) *Genetics and the Origin of Species* (Columbia Univ. Press, New York).
18. Kumar, S. & Subramanian, S. (2002) *Proc. Natl. Acad. Sci. USA* **99,** 803–808.
19. Li, W. H. (1997) *Molecular Evolution* (Sinauer, Sunderland, MA).
20. Isobe, T., Feigelson, E. D., Akritas, M. G. & Babu, G. J. (1990) *Astrophys. J.* **364,** 104–113.
21. Bromham, L. & Penny, D. (2003) *Nat. Rev. Genet.* **4,** 216–224.
22. Seino, S., Bell, G. I. & Li, W. H. (1992) *Mol. Biol. Evol.* **9,** 193–203.
23. Eastman, J. T. & McCune, A. R. (2000) *J. Fish Biol.* **57,** 84–102.
24. Kimura, M. (1983) *The Neutral Theory of Molecular Evolution* (Cambridge Univ. Press, Cambridge, U.K.).
25. Jablonski, D. (1993) *Nature* **364,** 142–144.
26. Flessa, K. W. & Jablonski, D. (1996) in *Evolutionary Paleobiology*, eds. Jablonski, D., Erwin, D. H. & Lipps, J. H. (Univ. of Chicago Press, Chicago), pp. 376–397.
27. Stehli, F. G., Douglas, D. G. & Newell, N. D. (1969) *Science* **164,** 947–949.
28. Allen, A. P., Brown, J. H. & Gillooly, J. F. (2002) *Science* **297,** 1545–1548.
29. Brown, J. H., Marquet, P. A. & Taper, M. L. (1993) *Am. Nat.* **142,** 573–584.